NASA TECHNICAL MEMORANDUM 107624

DETERMINATION OF STRESS INTENSITY FACTORS FOR INTERFACE CRACKS UNDER MIXED-MODE LOADING

Rajiv A. Naik and John H. Crews, Jr.

May 1992
To be presented at the ASTM National Symposium on Fracture Mechanics, June 30-July 2, 1992, Gatlinburg, TN

National Aeronautics and
Space Administration

Langley Research Center
Hampton, Virginia 23665

Abstract

A simple technique was developed using conventional finite element analysis to determine stress intensity factors (K_1 and K_2) for interface cracks under mixed-mode loading. This technique involves the calculation of crack-tip stresses using non-singular finite elements. These stresses are then combined and used in a linear regression procedure to calculate K_1 and K_2. The technique was demonstrated by calculating K_1 and K_2 for three different bimaterial combinations.

For the normal loading case, the calculated K_1 and K_2 were within 2.6% of an exact solution. The normalized K_1 and K_2 under shear loading were shown to be related to the normalized K_1 and K_2 under normal loading. Based on these relations a simple equation was derived for calculating K_1 and K_2 for mixed-mode loading from a knowledge of K_1 and K_2 under normal loading. Thus, for a given material combination and geometry, only one solution of K_1 and K_2 (under normal loading) is required to determine K_1 and K_2 over the full range of mixed-mode loading conditions.

The equation was verified by computing K_1 and K_2 for a mixed-mode case with equal normal and shear loading. The correlation between the exact and the finite element values was very good with errors of less than 3.7%.

This study provides a simple procedure to compute the K_2/K_1 ratio which can be used to characterize the stress state at the crack tip for various combinations of materials and loadings. Tests conducted over a range of K_2/K_1 ratios could be used to fully characterize interface fracture toughness.

Key Words: Bimaterial, finite element analysis, fracture mechanics, combined loading, phase angle.

Introduction

The performance of advanced composite materials is not only affected by their constituents but also by the character of the interface between the constituents. Interfacial cracking, either in the form of delamination or fiber-matrix debonding, is a typical failure mode in most classes of composite materials. Interfacial cracking, by definition, follows a predetermined path irrespective of the global loading. This, in conjunction with the mismatch between the material properties at the interface, leads to inherently mixed-mode crack growth. Unlike a crack in a homogeneous plate, mixed-mode conditions exist at an interface crack tip even for pure mode I loading. It is, therefore, important to characterize interfacial cracking over a range of mixed-mode conditions.

Linear elastic fracture mechanics (LEFM) concepts have been applied to the interface crack problem since 1959 when Williams [1] first determined that stresses oscillate near the tip of a semi-infinite interface crack. Other researchers [2-8] further examined the oscillatory behavior of the crack-tip stress and displacement fields and the resulting small contact region at a bimaterial crack. Rice and Sih [9] developed a solution for the stress intensity factors K_1 and K_2 for an interface crack between two semi-infinite plates subjected to a combination of both normal and shear loading.

Unlike K_I and K_{II}, the mode I and mode II stress intensity factors for a crack in a homogeneous material, bimaterial stress intensity factors K_1 and K_2 have some complicating properties that reflect on their usefulness in the development of fracture criteria [9]. For example, K_1 and K_2 are not strictly associated with opening and shear modes, respectively, as in the homogeneous case. Additionally, K_1 and K_2, as defined by Rice and Sih [9] and Hutchinson *et al.* [10], are functions of an arbitrary length parameter. Rice [11] noted the validity of the complex stress intensity factor K ($= K_1 + iK_2$, $i = \sqrt{-1}$) as a crack-tip characterizing parameter for cases of small scale nonlinear material behavior or small scale contact zones at the crack tip. Although K_1 and K_2 cannot be interpreted as mode I and mode II quantities it is possible to use the K_2/K_1 ratio to describe the stress state at the crack-tip.

Alternative definitions for the stress intensity factors were recently provided by Shih and Asaro [12] which eliminate the arbitrary length parameter and can be related to K_1 and K_2 in a simple way.

The strain energy release rate G was also examined by many researchers [13-16] as a another fracture parameter to characterize crack growth at a bimaterial interface. However, the mode I and mode II components of the strain energy release rate (G_I and G_{II}) are not well defined as was illustrated by Sun and Jih [17], Raju, *et al.* [18] and many other researchers. Recent studies [16, 19] have used the critical total strain energy release rate G_c to characterize interface fracture toughness and the K_2/K_1 ratio to describe the crack-tip stress state for the given test conditions. A complete characterization of interface toughness would then involve the determination of G_c over a range of K_2/K_1 ratios.

Closed-form methods for calculating K_1 and K_2 for interface crack problems are limited to a few special cases due to inherent mathematical difficulties. Numerical procedures are, therefore, required when K_1 and K_2 are desired for more general configurations and loadings. A boundary collocation method was used in [20] to generate interfacial K_1 and K_2 for a finite bimaterial plate. Special hybrid finite elements were developed in [21] and [22] to calculate K_1 and K_2. Conventional, non-singular finite elements were employed in [23] to calculate K_1 and K_2 from crack flank displacements and an extended form of the J-integral. The finite element method was also used together with domain integrals [11,24,25] to calculate K_1 and K_2. The finite element iterative method was used in [26] to evaluate K_1 and K_2 for a crack between dissimilar media. An eigenfunction expansion variational method was introduced in [27] to calculate K_1 and K_2. Each of the above mentioned numerical approaches requires its own computational scheme to handle the problem and has given satisfactory results.

In the present study, an alternative and convenient method of analysis is proposed for determining K_1 and K_2 under mixed-mode loading. First, a technique using the finite element method with non-singular elements was developed to calculate K_1 and K_2 under normal loading. K_1 and K_2 were calculated for three different material combinations: steel/aluminum,

aluminum/epoxy, and steel/epoxy, and compared with the classical solution to evaluate the technique. Next, simple relations were derived between the K_1 and K_2 due to normal and shear loading. These relations were used to derive simple equations to calculate K_1 and K_2 under mixed-mode loading from a knowledge of K_1 and K_2 under normal loading. The results from the simple equations were evaluated by comparing with finite element results for the mixed-mode case of equal normal and shear loading. The simple equations were then used to study the K_2/K_1 ratios for different material combinations over the full range of mixed-mode loading conditions.

Theoretical Background

Within the framework of LEFM, solutions for the singular stress fields at the crack-tip, the stress intensity factors and their relations to the strain energy release rates exist and are easily represented in concise form for an interfacial crack between two semi-infinite plates.

Consider a crack of length 2a lying along the interface of material 1 and material 2 (Fig. 1). The Young's moduli and Poisson's ratios of material 1 and 2 are given by E_1, ν_1, and E_2, ν_2, respectively. The coordinate system x-y-z has its origin at the center of the crack with the x-axis parallel to the interface and the y-axis normal to the interface. The distance r from the crack tip is measured along the interface. The body is remotely loaded by a uniform stress σ_{yy}^{∞} normal to the crack and a uniform shear stress σ_{xy}^{∞}. Only plane strain ($\varepsilon_{zz}=0$) deformations are considered.

For the configuration and loading shown in Fig. 1 the stresses along the interface directly ahead of the right crack tip can be written in complex notation as [10]

$$\sigma_{yy} + i\,\sigma_{xy} = \frac{(K_1 + i\,K_2)\,r^{i\varepsilon}}{\sqrt{2\pi r}}, \quad i = \sqrt{-1} \tag{1}$$

where K_1 and K_2 are the bimaterial stress intensity factors and ε is a bimaterial constant, also referred to as an oscillation index, given by [10]

$$\varepsilon = \frac{1}{2\pi} ln\left[\frac{G_1 + G_2(3 - 4\nu_1)}{G_2 + G_1(3 - 4\nu_2)}\right] \tag{2}$$

where G is the shear modulus and ν is Poisson's ratio. Subscripts 1 and 2 refer to material 1 and 2, respectively. Interchanging the properties of materials 1 and 2 leads to a change in sign of the bimaterial constant ε. In the present paper, the materials 1 and 2 were chosen such that E_2 was greater than E_1 which resulted in a positive value for ε.

Unlike a crack in a homogeneous body, the singularity for a crack at the bimaterial interface is of order $(-1/2 + i\,\varepsilon)$ as seen from Eq. (1). Also, the stress intensity factors K_1 and K_2 have units of (stress) x (length)$^{(1/2)}$ x (length)$^{-i\varepsilon}$. For the problem considered in Fig. 1, the complex stress intensity factor K $(= K_1 + iK_2)$ for the right crack tip is given by [10]

$$K = \sqrt{\pi a}\,(\sigma_{yy}^{\infty} + i\,\sigma_{xy}^{\infty})(1 + 2i\,\varepsilon)(2a)^{-i\,\varepsilon} \tag{3}$$

The complex K is often characterized by its magnitude $\left(\sqrt{K_1^2 + K_2^2}\right)$ and its phase angle ψ which is given by

$$\psi = \tan^{-1}\left(\frac{K_2}{K_1}\right) \tag{4}$$

Equations (3) and (4) can also be used to characterize the left crack tip (Fig. 1). However, to use the same equations, the reference coordinate axes x-y in Fig. 1 would have to be rotated by 180 degrees. In the rotated coordinate system materials 1 and 2 are reversed

leading to a sign change in ε. Thus the K_1 and K_2 for the left crack tip can be obtained by using $-\varepsilon$ in place of ε in Eq. (3).

As mentioned earlier, it was noted by Rice [12] that the small region of oscillations in the crack tip stresses can be ignored just as the inevitable small scale nonlinear material behavior at the crack tip in a homogeneous material is ignored in LEFM. The present study considered the stresses outside this small region of oscillations to determine K_1 and K_2.

For the configuration in Fig. 1, it can be shown from the classical solution in [10] that under shear loading the crack tip normal stresses, outside the small zone of oscillation, are tensile at the right crack tip whereas they are compressive at the left crack tip. Thus, the stress state at the right crack tip is more severe than at the left crack tip. The right crack tip was, therefore, considered in more detail in the present study.

Finite Element Analysis

The finite element mesh used in the present study is shown in Fig. 2. It consisted of four-noded isoparametric quadrilateral elements. The dimensions of the model were chosen to be large enough to preclude edge effects and adequately model semi-infinite plates as in Fig. 1. For the crack length-to-width ratio of 0.1 used here it was shown in [22] that the calculated stress intensity factors were not affected by the presence of the free edges. There were 2077 nodes and 1968 elements in the model and the analysis was performed using the MSC/NASTRAN code [28]. In the vicinity of the crack tip, a refined mesh was used (Fig. 2). The smallest elements with length Δ were next to the crack tip with element lengths doubling in the x- and y-directions. Plane strain conditions were imposed for all cases analyzed. Multi-point constraints were imposed along AB to enforce uniform ε_{xx} in order to simulate the infinite plate problem that was analyzed in [9]. The normal and shear loadings were imposed by displacement boundary conditions along the edges of the model and are listed in Table 1. Combinations of three different materials, aluminum, epoxy, and steel, were considered in the present study. The properties used for the three materials are given in Table 2.

The adequacy of the mesh refinement near the crack tip was evaluated in two ways. First, a convergence study was performed by analyzing a center crack in an infinite homogeneous plate problem. The same finite element model (Fig. 2) was used with $E_1 = E_2$ and $\nu_1 = \nu_2$. The computed nodal stresses and stress intensity factors (SIFs) under mode I and mode II loading were compared with existing handbook values [29]. The SIFs were determined by linear regression from a log-log plot of stress versus distance ahead of the crack tip as described later. For a mesh refinement of $\Delta/a = 5\text{x}10^{-6}$, the calculated SIFs were within 1% of the handbook values [29] for both mode I and mode II loading. Also, the slope of the log-log stress-distance plot near the crack tip was compared with the theoretical value of -0.5. In the region $1\text{x}10^{-5} \leq (r/a) \leq 2\text{x}10^{-2}$, its slope was -0.495.

To further evaluate the adequacy of this mesh refinement, the finite element model (Fig. 2) was used to analyze a crack at the interface of two dissimilar materials. For aluminum/epoxy, the computed nodal stresses near the crack tip were compared with the exact solution (Eq. (1)) for σ_{yy}^{∞} normal loading (Fig. 3) and for σ_{xy}^{∞} shear loading (Fig. 4). The σ_{xy} stresses under a normal loading are negative; $-\sigma_{xy}$ is plotted in Fig. 3 to show it on the log scale. The non-singular elements used in this analysis are not formulated to model the singularity at the crack tip. As a result, the stresses calculated from the first few elements next to the crack tip do not correlate well with the classical solution. However, in the region $1\text{x}10^{-4} \leq (r/a) \leq 2\text{x}10^{-2}$, there is a good correlation with the theoretical stresses for both loading conditions. Thus, the non-singular, isoparametric elements used in the present analysis were considered to be adequate for this study. The mesh refinement of $\Delta/a = 5\text{x}10^{-6}$ was used for all the cases analyzed.

The stress intensity factors K_1 and K_2 for the right crack tip were calculated using a simple procedure involving linear regression as described in the next section.

Procedure for Calculating K_1 and K_2

The normal σ_{yy} stresses and the shear σ_{xy} stresses directly ahead of the right crack tip are given by Eq. (1) and can be written explicitly (by separating real and imaginary parts) as

$$\sigma_{yy} = \frac{1}{\sqrt{2\pi r}}\{K_1 \cos(\varepsilon\, ln\,(r)) - K_2 \sin(\varepsilon\, ln\,(r))\}$$
$$\sigma_{xy} = \frac{1}{\sqrt{2\pi r}}\{K_1 \sin(\varepsilon\, ln\,(r)) + K_2 \cos(\varepsilon\, ln\,(r))\} \qquad (5)$$

By multiplying both sides of the σ_{yy} equation by $\cos(\varepsilon\, ln(r))$ and both sides of the σ_{xy} equation by $\sin(\varepsilon\, ln(r))$ and adding the resulting equations and denoting the "combined stress" by σ_1, we have

$$\sigma_1 = \sigma_{yy} \cos(\varepsilon\, ln\,(r)) + \sigma_{xy} \sin(\varepsilon\, ln\,(r)) = \frac{K_1}{\sqrt{2\pi r}} \qquad (6)$$

Similarly, by multiplying the σ_{yy} equation (Eq. (5)) by $-\sin(\varepsilon\, ln(r))$ and the σ_{xy} equation by $\cos(\varepsilon\, ln(r))$ and adding the two equations and denoting the combined stress by σ_2, we have

$$\sigma_2 = -\sigma_{yy} \sin(\varepsilon\, ln\,(r)) + \sigma_{xy} \cos(\varepsilon\, ln\,(r)) = \frac{K_2}{\sqrt{2\pi r}} \qquad (7)$$

The combined stresses σ_1 and σ_2 at nodes ahead of the crack tip were determined from the computed σ_{yy} and σ_{xy} stresses from the finite element analysis. It is clear from Eqs. (6) and (7) that plots of σ_1 and σ_2 with distance r on a log-log scale will be straight lines with a slope of -0.5. The stress intensity factors K_1 and K_2 were calculated from a linear regression fit of slope -0.5 to the $\log(\sigma_1)$ versus $\log(r)$ and $\log(\sigma_2)$ versus $\log(r)$ curves, respectively.

If either σ_1 or σ_2 is computed to be a negative quantity, then the corresponding K_1 or K_2 will have a negative sign. The sign of σ_1 and σ_2 was ignored while using the linear regression procedure. The calculated K_1 or K_2 was then assigned a negative sign if the corresponding σ_1 or σ_2 had a negative sign.

As mentioned earlier, the non-singular elements next to the crack tip do not model singular behavior. Thus, the combined stresses σ_1 and σ_2 from the first two or three elements will not lie on a line with a slope of -0.5 on a log-log plot of σ_1 and σ_2 with distance r. Also, the combined stresses from elements away from the crack tip outside the singularity-dominated region will not lie on a line with a slope of -0.5.

The linear regression fit for calculating K_1 and K_2 was performed in the region where the $\log(\sigma_1)$ versus log(r) and $\log(\sigma_2)$ versus log(r) curves had a slope of -0.5. This regression region was determined by the following procedure: the slopes of the log-log plots of σ_1 and σ_2 versus r were determined for successive pairs of nodes ahead of the crack starting from the node at the crack tip. The pairs of nodes for which this slope was -0.5 ± 0.01 were included in the regression region and the combined stresses σ_1 and σ_2 from these nodes were used in the calculation of K_1 and K_2. This procedure was used to calculate K_1 and K_2 for the normal and the mixed-mode loading cases analyzed in this study.

Relations Between K_1 and K_2 under Normal and Shear Loading

In order to investigate the properties of K_1 and K_2 under normal and shear loading it is instructive to examine the crack-tip stresses for these two loading cases. Figure 5 shows the normalized crack-tip stresses for these two loadings calculated for the aluminum/epoxy case based on the classical solution given in [10]. It is clear from Fig. 5 that the crack-tip stresses obey the following relations:

$$\frac{(\sigma_{yy})_{Normal}}{\sigma^{\infty}_{yy}} = \frac{(\sigma_{xy})_{Shear}}{\sigma^{\infty}_{xy}} \quad \text{and} \quad \frac{(\sigma_{xy})_{Normal}}{\sigma^{\infty}_{yy}} = -\frac{(\sigma_{yy})_{Shear}}{\sigma^{\infty}_{xy}} \tag{8}$$

Using the relations in Eq. (8) together with Eq. (5) we have

$$\begin{aligned}
&\{(K_{1N})_{Normal}\cos(\varepsilon\, ln\,(r)) - (K_{2N})_{Normal}\sin(\varepsilon\, ln\,(r))\} = \\
&\qquad \{(K_{1N})_{Shear}\sin(\varepsilon\, ln\,(r)) + (K_{2N})_{Shear}\cos(\varepsilon\, ln\,(r))\} \\
&\text{and} \qquad (9) \\
&\{(K_{1N})_{Normal}\sin(\varepsilon\, ln\,(r)) + (K_{2N})_{Normal}\cos(\varepsilon\, ln\,(r))\} = \\
&\qquad \{-(K_{1N})_{Shear}\cos(\varepsilon\, ln\,(r)) + (K_{2N})_{Shear}\sin(\varepsilon\, ln\,(r))\}
\end{aligned}$$

where

$$(K_{1N})_{Normal} = \frac{(K_1)_{Normal}}{\sigma^{\infty}_{yy}} \quad \text{and} \quad (K_{2N})_{Normal} = \frac{(K_2)_{Normal}}{\sigma^{\infty}_{yy}} \tag{10}$$

are the normalized stress intensity factors for the right crack tip under pure normal loading and

$$(K_{1N})_{Shear} = \frac{(K_1)_{Shear}}{\sigma^{\infty}_{xy}} \quad \text{and} \quad (K_{2N})_{Shear} = \frac{(K_2)_{Shear}}{\sigma^{\infty}_{xy}} \tag{11}$$

are the normalized stress intensity factors for the right crack tip under pure shear loading. By multiplying both sides of the first equation (Eq. (9)) by $\cos(\varepsilon\, ln(r))$ and both sides of the second equation (Eq. (9)) by $\sin(\varepsilon\, ln(r))$ and adding the resulting equations we have the following relation between the normalized stress intensity factors:

$$(K_{1N})_{Normal} = (K_{2N})_{Shear} \tag{12}$$

Similarly, by multiplying both sides of the first equation (Eq. (9)) by -sin(ε *ln*(r)) and both sides of the second equation (Eq. (9)) by cos(ε *ln*(r)) and adding the resulting equations we have the following relation between the normalized stress intensity factors:

$$(K_{2N})_{Normal} = -(K_{1N})_{Shear} \tag{13}$$

The relations in Eqs. (12) and (13) are valid for both the right and the left crack tips for the configuration in Fig. 1. Although the relations in Eqs. (12) and (13) were derived from the equations for the crack-tip stresses for the center crack configuration in Fig. 1, they are also valid for the semi-infinite crack problem with point loading on the crack faces.

The relations in Eqs. (12) and (13) can also be derived by expanding Eq. (3) into real and imaginary parts and examining the expressions for the normalized K_1 and K_2 under normal and shear loading. For normal loading we have

$$\begin{aligned}(K_{1N})_{Normal} &= \sqrt{\pi a}\,\{\cos(\varepsilon\, ln\,(2a)) + 2\varepsilon\,\sin(\varepsilon\, ln\,(2a))\} \\ (K_{2N})_{Normal} &= \sqrt{\pi a}\,\{-\sin(\varepsilon\, ln\,(2a)) + 2\varepsilon\,\cos(\varepsilon\, ln\,(2a))\}\end{aligned} \tag{14}$$

and for shear loading we have

$$\begin{aligned}(K_{1N})_{Shear} &= \sqrt{\pi a}\,\{-2\varepsilon\,\cos(\varepsilon\, ln\,(2a)) + \sin(\varepsilon\, ln\,(2a))\} \\ (K_{2N})_{Shear} &= \sqrt{\pi a}\,\{2\varepsilon\,\sin(\varepsilon\, ln\,(2a)) + \cos(\varepsilon\, ln\,(2a))\}\end{aligned} \tag{15}$$

An examination of Eqs. (14) and (15) confirms the validity of the relations derived in Eqs. (12) and (13).

The K_1 and K_2 under mixed-mode loading can be obtained by expanding Eq. (3) into real and imaginary parts and using Eqs. (14) and (15) as

$$\begin{aligned} K_1 &= \sigma_{yy}^{\infty} (K_{1N})_{Normal} + \sigma_{xy}^{\infty} (K_{1N})_{Shear} \\ K_2 &= \sigma_{yy}^{\infty} (K_{2N})_{Normal} + \sigma_{xy}^{\infty} (K_{2N})_{Shear} \end{aligned} \tag{16}$$

Using Eq. (16) and the relations in Eqs. (12) and (13) the K_1 and K_2 under any combination of normal and shear loading can be written as

$$\begin{aligned} K_1 &= \sigma_{yy}^{\infty} (K_{1N})_{Normal} - \sigma_{xy}^{\infty} (K_{2N})_{Normal} \\ K_2 &= \sigma_{yy}^{\infty} (K_{2N})_{Normal} + \sigma_{xy}^{\infty} (K_{1N})_{Normal} \end{aligned} \tag{17}$$

Thus, if $(K_{1N})_{Normal}$ and $(K_{2N})_{Normal}$ are known for a particular material combination and crack length, then K_1 and K_2 under any combination of normal and shear loading can be determined by using Eq. (17).

Equations (17) can be used to generate K_1 and K_2 values for a range of mixed-mode loadings for both the right and the left crack tips based on a knowledge of the corresponding $(K_{1N})_{Normal}$ and $(K_{2N})_{Normal}$. The K_2/K_1 ratio, or $\tan(\psi)$ (see Eq. (4), for mixed-mode loading can be expressed in terms of the ratio $(K_2/K_1)_{Normal}$ by using Eq. (17) as

$$\tan(\psi) = \frac{K_2}{K_1} = \frac{\left[(K_2 / K_1)_{Normal} + (\sigma_{xy}^{\infty} / \sigma_{yy}^{\infty})\right]}{\left[1 - (\sigma_{xy}^{\infty} / \sigma_{yy}^{\infty})(K_2 / K_1)_{Normal}\right]} \tag{18}$$

As $(\sigma_{xy}^{\infty} / \sigma_{yy}^{\infty})$ approaches $\pm\infty$, the pure shear loading case, it can be shown that the right hand side of Eq. (18) approaches a limiting value of $-(K_1/K_2)_{Normal}$. Thus, Eq. (18) provides

a means of calculating the (K_2/K_1) ratio or $\tan(\psi)$ over the full range of mixed-mode ratios from a knowledge of K_1 and K_2 for the normal loading case.

Equation (18) is valid for both the right and the left crack tips. However, the appropriate $(K_2/K_1)_{Normal}$ ratio should be used in Eq. (18). For the left crack tip K_1 and K_2 under normal loading can be calculated from a knowledge of K_1 and K_2 for the right crack tip. By using $-\varepsilon$ in the place of ε in Eq. (14) it can be shown that under normal loading the ratio of the stress intensity factors at the left crack tip is equal to $-(K_2/K_1)$ where K_1 and K_2 are the stress intensity factors at the right crack tip.

Results and Discussion

The finite element analysis and procedure described above were used to calculate K_1 and K_2 for three different material combinations: aluminum/epoxy, steel/epoxy, and steel/aluminum. Two different loading conditions were analyzed: normal loading ($\sigma_{xy}^{\infty} = 0$) and mixed-mode loading with $\sigma_{yy}^{\infty} = \sigma_{xy}^{\infty}$. In all cases the half-crack length, a, was 20 units. The K_2/K_1 ratios were plotted for a range of mixed-mode load ratios using Eq. (18).

Figure 6 shows normalized combined stresses σ_1 and σ_2 for the normal loading case as a function of normalized distance from the crack tip on a log-log plot. The circular symbols indicate the locations at which nodal stresses were available from the finite element analysis. Note that the σ_2 combined stress was a negative quantity and $-\sigma_2$ was plotted on the log scale in the figure. The negative σ_2 also led to a negative K_2. There was very little difference between the calculated σ_1 values for the three material combinations which led to similar K_1 values (Table 3). However, there was some difference between the calculated σ_2 values leading to larger differences between the calculated K_2 values for the different material combinations (Table 3). As mentioned earlier, the results from the first few elements do not lie on a straight line with a slope of -0.5. The appropriate regression region for calculating K_1 and K_2 was determined as described earlier and was found to be $1.6\text{x}10^{-4} \leq (r/a) \leq 1\text{x}10^{-2}$. Table 3 shows a comparison between the exact [10] and the calculated normalized K_1 and K_2 for normal

loading. There was excellent agreement between the calculated and the exact [10] K_1 and K_2 with errors of less than 2.6%. As the mismatch between the material properties decreased, the K_2 values became smaller with larger errors in the calculated values.

The mixed-mode loading case was analyzed to verify the relations derived in Eq. (17) for calculating K_1 and K_2 from a knowledge of K_{1N} and K_{2N} under normal loading. Values for K_{1N} and K_{2N} under normal loading were taken from Table 3 (exact solution). These were used together with the relations in Eq. (17) to calculate K_1 and K_2 (see Table 4) for the $\sigma_{yy}^{\infty} = \sigma_{xy}^{\infty}$ mixed-mode case. These results were compared with results calculated from the finite element analysis. The nodal stresses ahead of the crack tip for the mixed-mode loading case were obtained by superposing the nodal stresses from the pure normal and pure shear loading cases. The regression region for this case was also found to be $1.6 \times 10^{-4} \leq (r/a) \leq 1 \times 10^{-2}$. The excellent correlation (errors less than 3.7%) between the results using Eq. (17) and the finite element method (FEM) verifies the derivations in the previous section. The crack-tip stresses for the two extreme loading cases of pure normal and pure shear loading were verified earlier (Figs. 3 and 4) by comparing with the exact solution [10].

Figures 7 and 8 show plots of the K_2/K_1 ratios using Eq. (18) for two different ranges of mixed-mode loading ratios. Figure 7 shows the normal-load dominated cases with mixed-mode loading ratios ranging from 0 to 1.0. The $(K_2/K_1)_{Normal}$ ratios used were obtained from the exact solution [10] in Table 3. Two limiting material combinations are also included for reference purposes. The crack in a large homogeneous plate represents a bimaterial case with no mismatch in material properties ($\varepsilon=0$). For this case the K_2/K_1 ratio is equivalent to the ratio of classical mode II and mode I stress intensity factors, K_{II} and K_I, respectively. The rigid/epoxy case represents a case in which the mismatch between the properties is characterized by a relatively large value of the bimaterial constant, $\varepsilon=0.094$. The K_2/K_1 curves for all cases fell between the two extremes represented by these two limiting cases; cases with the larger material property mismatch were closer to the rigid/epoxy case. For the

mode I loading case ($\sigma^{\infty}_{xy} / \sigma^{\infty}_{yy} = 0$), the K_2/K_1 ratio is negative due to the presence of a negative shear stress at the crack tip (Fig. 3). For mixed-mode ratios between 0.0 and 0.5, the K_2/K_1 ratio increases linearly with approximately the same slope as the homogeneous crack case. Unlike the homogeneous crack case, the K_2/K_1 ratios for the bimaterial cases under equal normal and shear loading ($\sigma^{\infty}_{xy} / \sigma^{\infty}_{yy} = 1$) have values less than 1.0 (Fig. 7). This is due to the negative shear stress (Fig. 3) at the crack tip, which under normal loading subtracts from the positive shear stress (Fig. 4) under shear loading.

Figure 8 show plots of the K_2/K_1 ratios from Eq. (18) over the full range of mixed-mode loading but with an emphasis on the shear dominated cases. For the shear dominated loading, the curves are highly nonlinear and there is significant departure from the homogeneous case. The nonlinearity in the curves can be explained by examining Eq. (18) for the aluminum/epoxy case ($K_2/K_1 = -0.11$). For this case, the denominator in Eq. (18) becomes more dominant for mixed-mode ratios greater than 1 and, thus, leads to the nonlinearity in the curves. For pure mode II loading the (K_2/K_1) ratios approach a limiting value of $-(K_1/K_2)_{Normal}$ as discussed earlier.

Fracture toughness of the interface between two different materials can be characterized by measuring the critical strain energy release rate G_c over a range of K_2/K_1 ratios. The present study provides a simple equation (Eq. (18)) to determine these values for the (K_2/K_1) ratios over the full range of mixed-mode loadings if the $(K_2/K_1)_{Normal}$ ratio under normal loading is known. The $(K_2/K_1)_{Normal}$ ratio for any configuration can be determined using conventional, non-singular finite elements and the simple regression procedure developed in this study.

Concluding Remarks

A simple technique was developed using conventional finite element analysis to determine stress intensity factors for interface cracks under mixed-mode loading. This technique involved the calculation of crack-tip stresses using non-singular finite elements.

These stresses were then combined and used in a linear regression procedure to calculate interface stress intensity factors K_1 and K_2 . The technique was demonstrated by calculating K_1 and K_2 for three different bimaterial combinations. The nature of the stress intensity factors K_1 and K_2 was studied over the full range of mixed-mode loadings and compared to the limiting cases of a crack in a homogeneous plate and a bimaterial crack at the interface of a rigid substrate and epoxy.

For the normal loading case, the calculated K_1 and K_2 were within 2.6% of an exact solution. The normalized K_1 and K_2 under shear loading were shown to be related to the normalized K_1 and K_2 under normal loading. Based on these relations a simple equation was derived for calculating K_1 and K_2 for mixed-mode loading from a knowledge of K_1 and K_2 under normal loading. Thus, for a given material combination and crack length, only one solution of K_1 and K_2 under normal loading is required to determine K_1 and K_2 over the full range of mixed-mode loading conditions.

This equation was verified by computing K_1 and K_2 for a mixed-mode case with equal normal and shear loading. Once again the correlation between the classical and the finite element values was very good with errors of less than 3.7%.

This study provides a simple procedure to compute the K_2/K_1 ratio which can be used to characterize the stress state at the crack tip for various combinations of materials and loadings. Tests conducted over a range of K_2/K_1 ratios could be used to fully characterize interface fracture toughness.

References

1. Williams, M. L.; "The Stresses Around a Fault or Crack in Dissimilar Media," *Bull. Seismol. Soc. America*, Vol. 49, No. 2, April 1959, pp. 199-204.
2. England, A. H.; "A Crack Between Dissimilar Media," *J. Appl. Mech.*, Vol. 32, June 1965, pp. 400-402.
3. Erdogan, F.; "Stress Distribution in Bonded Dissimilar Materials with Cracks," *J. Appl. Mech.*, Vol. 32, June 1965, pp. 403-410.
4. Cherepanov, G. P.; *Mechanics of Brittle Fracture*, McGraw-Hill, New York, 1979.
5. Comninou, M.; "The Interface Crack," *J. Appl. Mech.*, Vol. 44, Dec. 1977, pp. 631-636.
6. Clements, D. L.; "A Crack Between Dissimilar Anisotropic Media," *Int. J. Eng. Sc.*, Vol. 9, 1971, pp. 257-265.
7. Gautesen, A. K. and Dundurs, J.; "The Interface Crack in a Tension Field," *J. Appl. Mech.*, Vol. 54, March 1987, pp. 93-98.
8. Wang, S. S. and Choi, I.; "The Interface Crack Between Dissimilar Anisotropic Composite Materials," *J. Appl. Mech.*, Vol. 50, March 1983, pp. 169-178.
9. Rice, J. R. and Sih, G. C.; "Plane Problems of Cracks in Dissimilar Media," *J. Appl. Mech.*, June 1965, pp. 418-423.
10. Hutchinson, J. W., Mear, M. E., and Rice, J. R.; "Crack Paralleling an Interface Between Dissimilar Materials," *J. of Appl. Mech.*, Vol. 54, Dec. 1987, pp. 828-832.
11. Rice, J. R.; "Elastic Fracture Mechanics Concepts for Interfacial Cracks," *J. of Appl. Mech.*, Vol. 55, March 1988, pp. 98-103.
12. Shih, C. F. and Asaro, R. J.; "Elastic-Plastic Analysis of Cracks on Bimaterial Interfaces: Part I - Small Scale Yielding," *J. of Appl. Mech.*, Vol. 55, June 1988, pp. 299-316.
13. Malyshev, B. M. and Salganik, R. L.; "The Strength of Adhesive Joints Using the Theory of Cracks," *Int. J. Frac. Mech.*, Vol. 1, 1965, pp. 114-128.

14. Anderson, G. P., Devries, K. L., and Williams, M. L.; "Mixed Mode Stress Field Effect in Adhesive Fracture," *Int. J. Frac.*, Vol. 10, 1970, pp. 565-583.

15. Mulville, D. R., Hunston, D. L., and Mast, P. W.; "Developing Failure Criteria for Adhesive Joints Under Complex Loading," *J. Eng. Mat. Tech.*, Vol. 100, Jan. 1978, pp. 25-31.

16. Evans, A. G., Ruhle, M., Dalgleish, B. J., and Charalambides, P. G.; "The Fracture Energy of Bimaterial Interfaces," *Metall. Trans. A*, Vol. 21A, Sept. 1990, pp. 2419-2429.

17. Sun, C. T. and Jih, C. J.; "On Strain Energy Release Rates for Interfacial Cracks in Bi-Material Media," *Eng. Frac. Mech.*, Vol. 28, No. 1, 1987, pp. 13-20.

18. Raju, I. S., Crews, J. H., and Aminpour, M. A.; "Convergence of Strain Energy Release Rate Components for Edge-Delaminated Composite Laminates," *Eng. Frac. Mech.*, Vol. 30, No. 3, 1988, pp. 383-396.

19. Suo, Z. and Hutchinson, J. W.; "Sandwich Test Specimens for Measuring Interface Crack Toughness," *Mater. Sci. Eng.*, Vol. A107, 1989, pp. 135-143.

20. Sawyer, S. G. and Anderson, R. B.; "Collocated Interfacial Stress Intensity Factors for Finite Bi-Material Plates," *Eng. Frac. Mech.*, Vol. 4, 1972, pp. 605-616.

21. Lin, K. Y. and Mar, J. W.; "Finite Element Analysis of Stress Intensity Factors for Cracks at a Bi-Material Interface," *Int. J. Frac.*, Vol. 12, No. 4, August 1976, pp. 521-531.

22. Staab, G. H. and Chang, T. C.; "A Finite Element Analysis of the Mixed Mode Bi-Material Fracture Mechanics Problem," *Comp. & Struct.*, Vol. 18, No. 5, 1984, pp. 853-859.

23. Smelser, R. E.; "Evaluation of Stress Intensity Factors for Bimaterial Bodies Using Numerical Crack Flank Displacement Data," *Int. J. Frac.*, Vol. 15, No. 2, April 1979, pp. 135-143.

24. Hong, C-C. and Stern, M.; "The Computation of Stress Intensity Factors in Dissimilar Materials," *J. Elas.*,Vol. 8, No. 1, Jan. 1978, pp. 21-34.

25. Wang, S. S. and Yau, J. F.; "Interface Cracks in Adhesively Bounded Lap-Shear Joints," *Int. J. Frac.*, Vol. 19, 1982, pp. 295-309.

26. Barsoum, R. S.; "Application of the Finite Element Iterative Method to the Eigenvalue Problem of a Crack Between Dissimilar Media," *Int. J. Num. Meth. Eng.*, Vol. 26, 1988, pp. 541-554.

27. Wang, W-C. and Chen, J-T.; "Variational Analysis of Interfacial Stress Intensity Factors for Finite Bimaterial Plates under Biaxial Load," *Comp. Struct.*, Vol. 17, 1991, pp. 157-179.

28. MSC/NASTRAN User's Manual, Vols. 1 and 2, Nov. 1989. The MacNeal-Schwendler Corporation, Los Angeles, California.

29. Tada, H., Paris, P. C., and Irwin, G.; *The Stress Analysis of Crack Handbook*, 2nd Edition, Paris Production Incorporated (and Del Research Corporation), St. Louis, Missouri, 1985.

Table 1 -- Displacement boundary conditions for normal and shear loading.

Loading	Boundary condition at			
	x = 0	x = 10a	y = -30a	y = 30a
Normal	u = 0	u = const.[a]	v = 0	v = 1
Shear	v = 0	v = (1/3)	u = 0	u = 1

[a]A constant displacement was imposed using multi-point constraints.

Table 2 -- Material properties used in the analysis.

Property	Aluminum	Epoxy	Steel
Young's modulus, E (GPa)	68.95	3.10	206.85
Poisson's Ratio, ν	0.30	0.35	0.30

Table 3 -- Comparison of interface stress intensity factors under σ_{yy}^{∞} normal loading.

Bimaterial	ε	$K_1/(\sigma_{yy}^{\infty}\sqrt{\pi a})$		$K_2/(\sigma_{yy}^{\infty}\sqrt{\pi a})$	
		Ref. [10]	Present	Ref. [10]	Present
Steel/Aluminum	0.046	1.001	0.991	-0.078	-0.080
Aluminum/Epoxy	0.067	1.002	0.996	-0.115	-0.116
Steel/Epoxy	0.072	1.003	0.996	-0.124	-0.126

Table 4 -- Comparison of interface stress intensity factors for mixed-mode loading ($\sigma_{yy}^{\infty} = \sigma_{xy}^{\infty} = \sigma_o$).

Bimaterial	ε	$K_1/(\sigma_o\sqrt{\pi a})$		$K_2/(\sigma_o\sqrt{\pi a})$	
		Eq. [17]	FEM	Eq. [17]	FEM
Steel/Aluminum	0.046	1.079	1.056	0.923	0.929
Aluminum/Epoxy	0.067	1.117	1.076	0.888	0.892
Steel/Epoxy	0.072	1.127	1.098	0.879	0.882

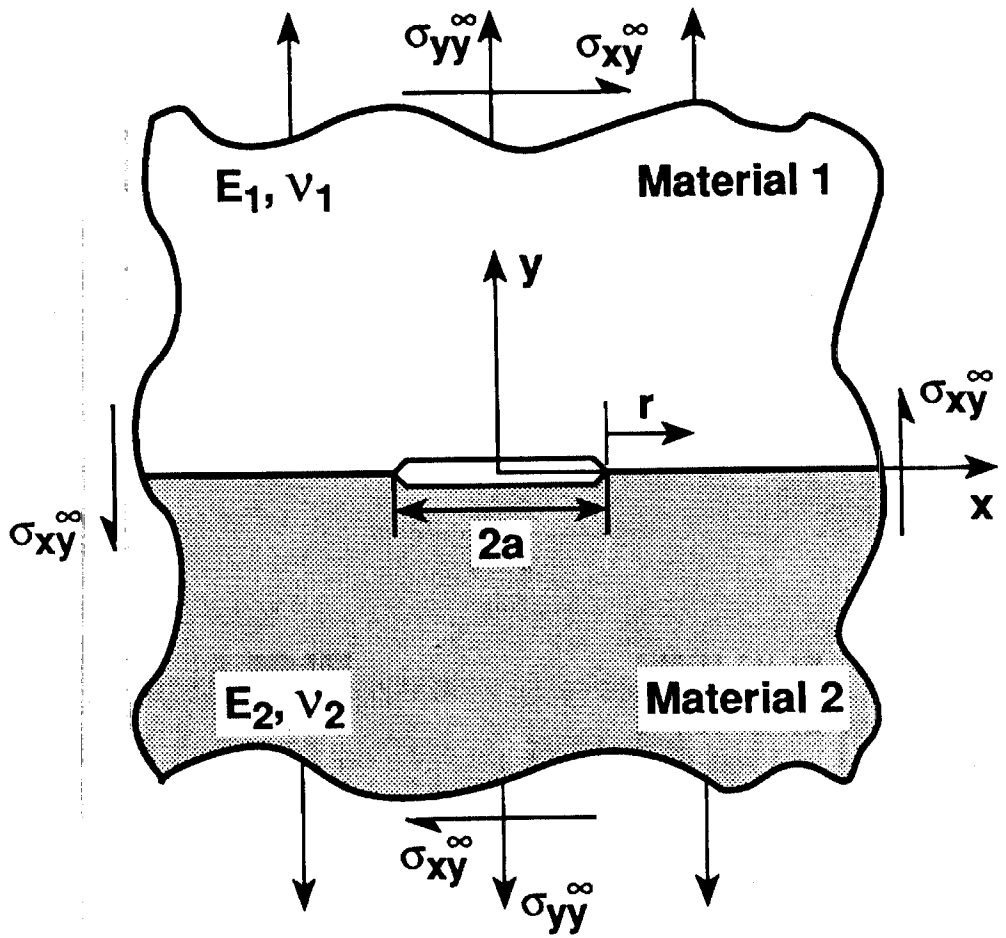

Fig. 1 -- Configuration and loading for a bimaterial crack.

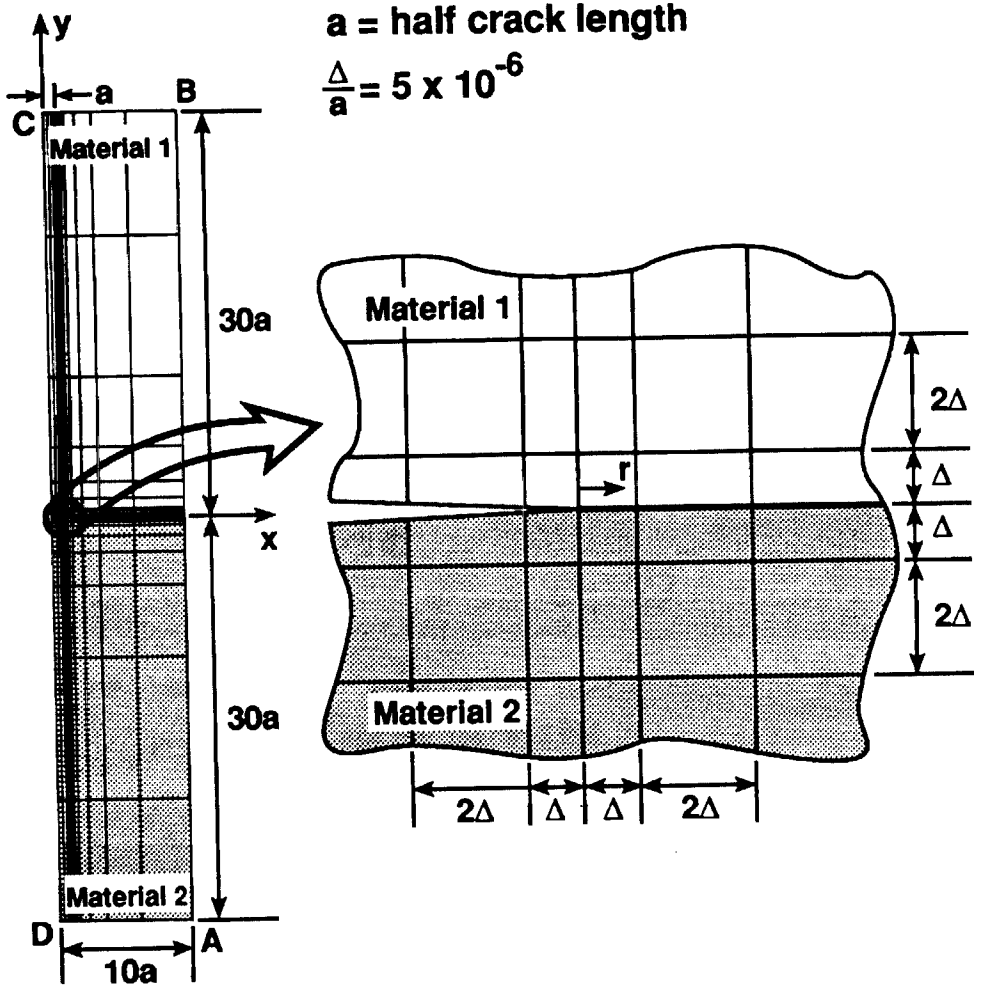

Fig. 2 -- Finite element model showing mesh detail at crack tip.

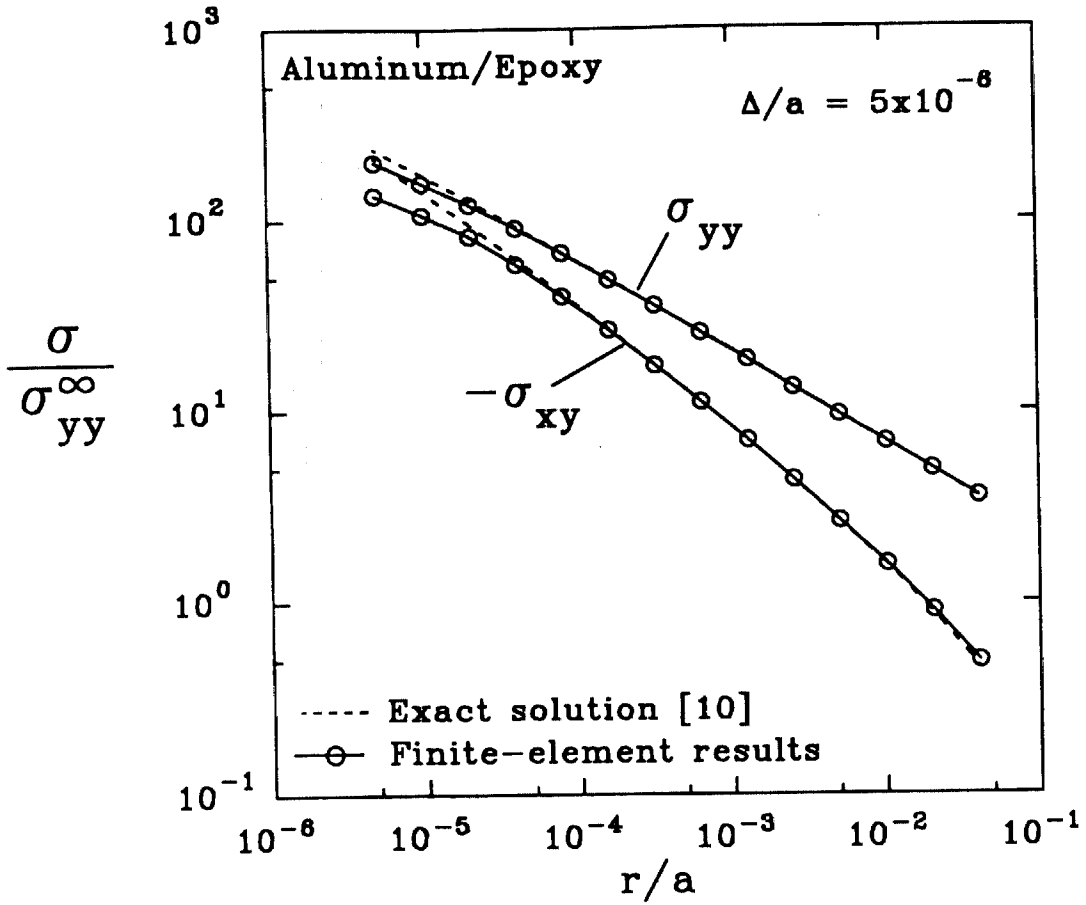

Fig. 3 -- Comparison of crack-tip stresses for normal loading.

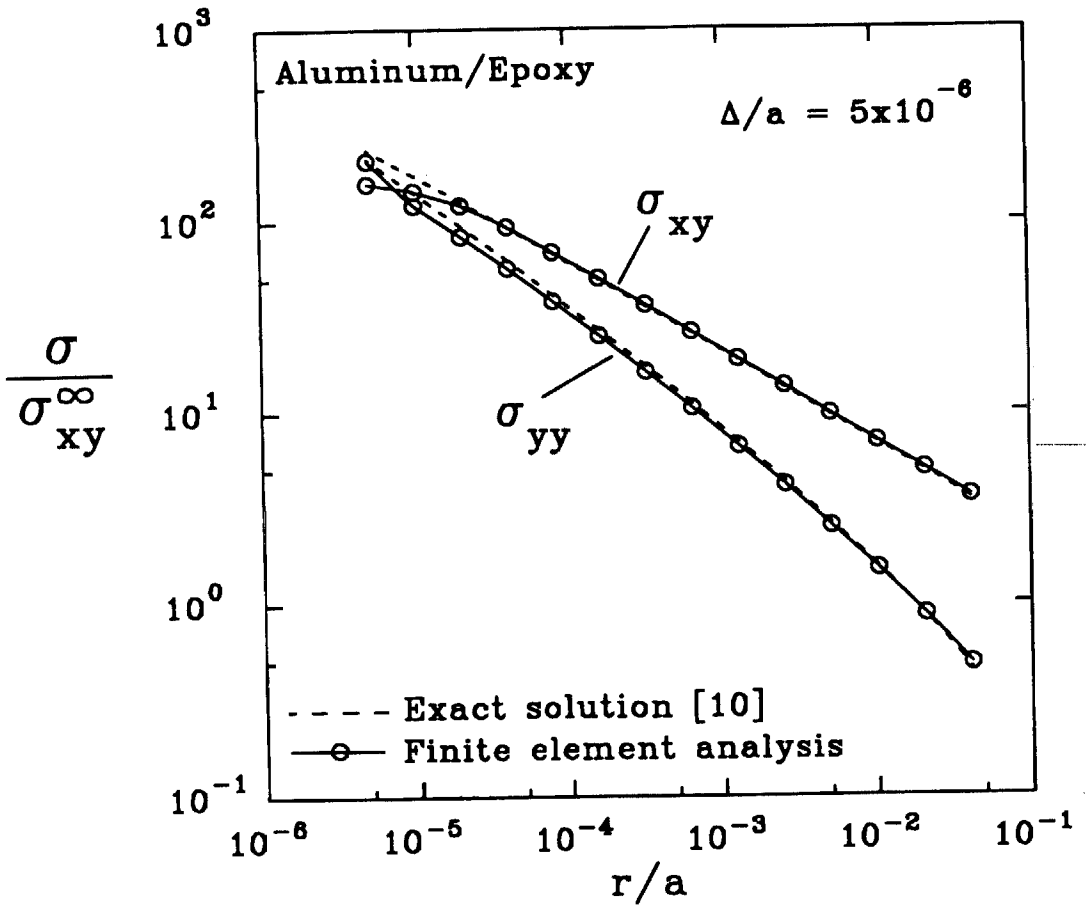

Fig. 4 -- Comparison of crack-tip stresses for shear loading.

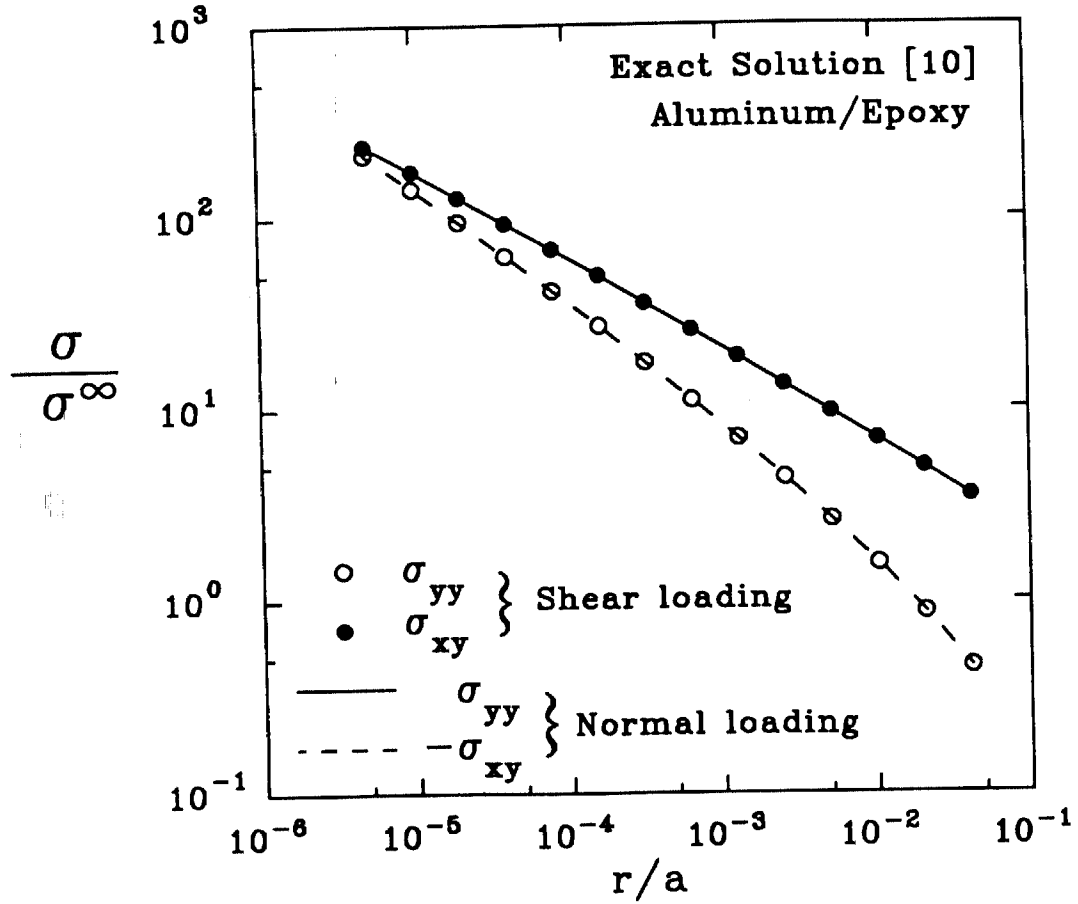

Fig. 5 -- Relations between crack-tip stresses for normal and shear loading.

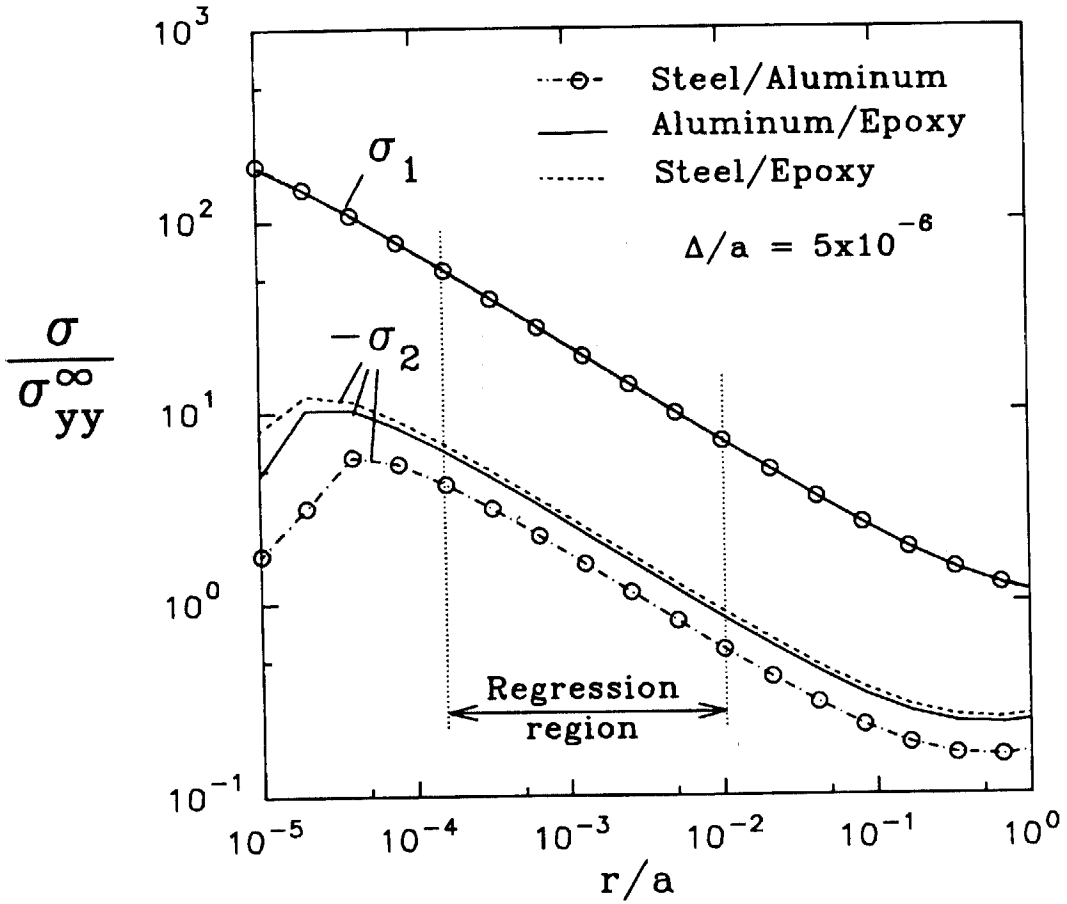

Fig. 6 -- Combined stresses at crack tip under normal loading.

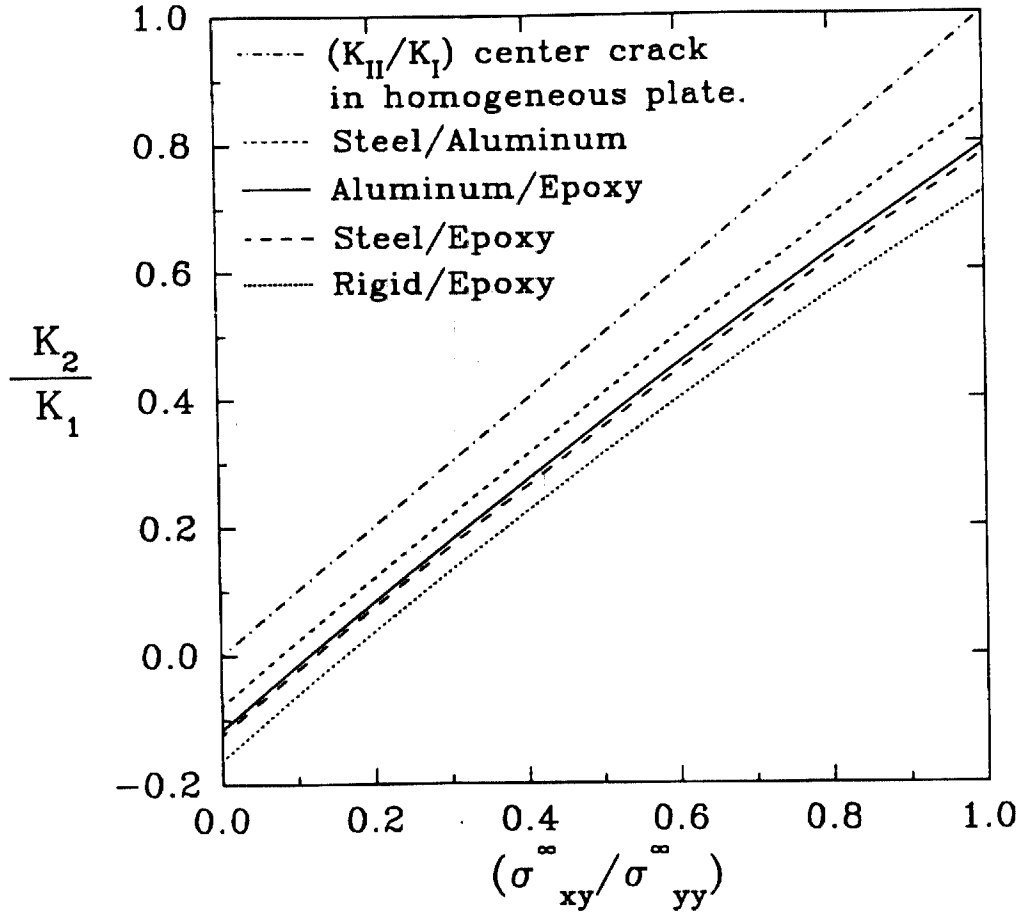

Fig. 7 -- K_2/K_1 ratios for mixed-mode ratios less than 1.0.

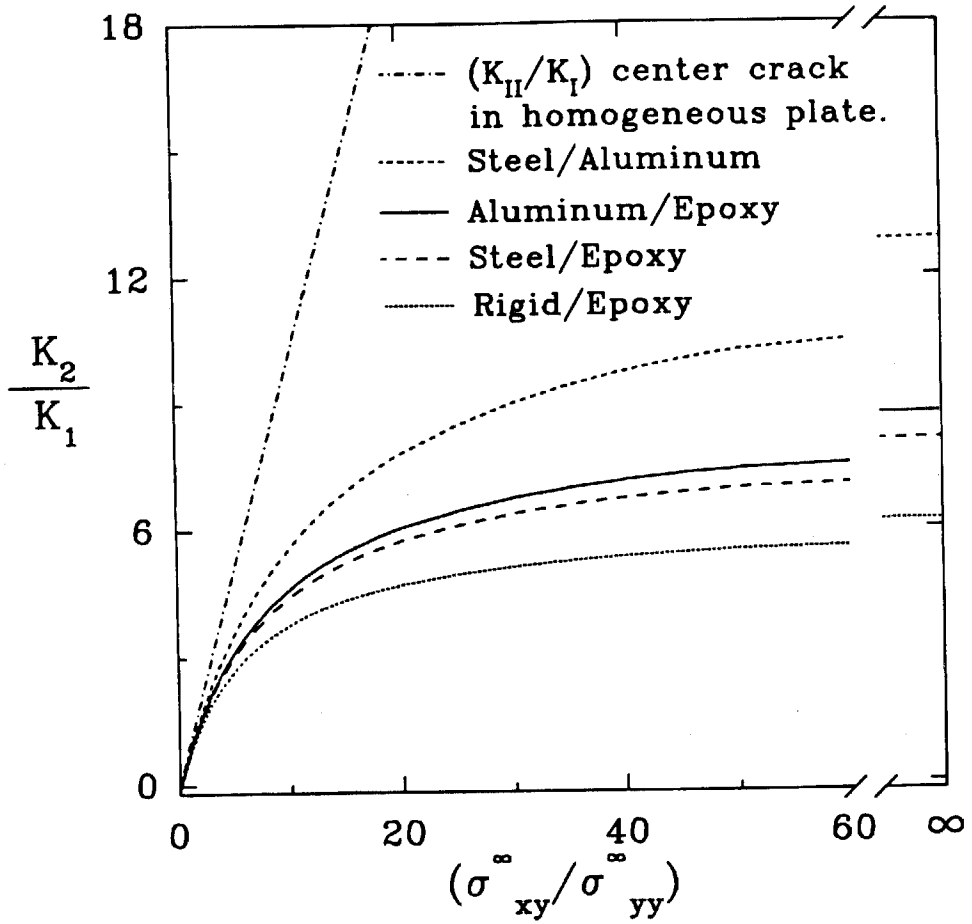

Fig. 8 -- K_2/K_1 ratios over full range of mixed-mode load ratios.

REPORT DOCUMENTATION PAGE

Form Approved
OMB No. 0704-0188

1. AGENCY USE ONLY (Leave blank)	2. REPORT DATE	3. REPORT TYPE AND DATES COVERED
	May 1992	Technical Memorandum

4. TITLE AND SUBTITLE

Determination of Stress Intensity Factors for Interface Cracks Under Mixed-Mode Loading

5. FUNDING NUMBERS

505-63-50-04

6. AUTHOR(S)

Rajiv A. Naik and John H. Crews, Jr.

7. PERFORMING ORGANIZATION NAME(S) AND ADDRESS(ES)

NASA Langley Research Center
Hampton, VA 23665-5225

8. PERFORMING ORGANIZATION REPORT NUMBER

9. SPONSORING/MONITORING AGENCY NAME(S) AND ADDRESS(ES)

National Aeronautics and Space Administration
Washington, DC 20546

10. SPONSORING/MONITORING AGENCY REPORT NUMBER

NASA TM-107624

11. SUPPLEMENTARY NOTES

Naik: Analytical Services and Materials, Inc., NASA Langley Research Center, Hampton, VA 23665-5225;
Crews: NASA Langley Research Center, Hampton, VA 23665-5225

12a. DISTRIBUTION/AVAILABILITY STATEMENT

Unclassified - Unlimited

Subject Category - 24

12b. DISTRIBUTION CODE

13. ABSTRACT *(Maximum 200 words)*

A simple technique was developed using conventional finite-element analysis to determine stress intensity factors (K_1 and K_2) for interface cracks under mixed-mode loading. This technique involves the calculation of crack-tip stresses using non-singular finite elements. These stresses are then combined and used in a linear regression procedure to calculate K_1 and K_2. The technique was demonstrated by calculating K_1 and K_2 for three different bimaterial combinations.

For the normal loading case, the calculated K_1 and K_2 were within 2.6 percent of an exact solution. The normalized K_1 and K_2 under shear loading were shown to be related to the normalized K_1 and K_2 under normal loading. Based on these relations a simple equation was derived for calculating K_1 and K_2 for mixed-mode loading from a knowledge of K_1 and K_2 under normal loading. Thus, for a given material combination and geometry, only one solution of K_1 and K_2 (under normal loading) is required to determine K_1 and K_2 over the full range of mixed-mode loading conditions.

The equation was verified by computing K_1 and K_2 for a mixed-mode case with equal normal and shear loading. The correlation between the exact and the finite-element values was very good with errors of less than 3.7 percent.

This study provides a simple procedure to compute the K_2/K_1 ratio which can be used to characterize the stress state at the crack tip for various combinations of materials and loadings. Tests conducted over a range of K_2/K_1 ratios could be used to fully characterize interface fracture toughness.

14. SUBJECT TERMS

Bimaterial; Finite element analysis; Fracture mechanics; Combined loading; Phase angle

15. NUMBER OF PAGES

30

16. PRICE CODE

A03

17. SECURITY CLASSIFICATION OF REPORT	18. SECURITY CLASSIFICATION OF THIS PAGE	19. SECURITY CLASSIFICATION OF ABSTRACT	20. LIMITATION OF ABSTRACT
Unclassified	Unclassified		